

# Independent Set Enumeration and Estimation of Related Constants of Grid Graphs

Kai Liang

July 8, 2025

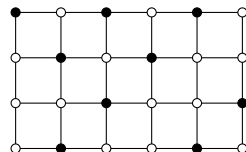
## Abstract

We employed tensor network contraction algorithms to compute the hard-core lattice gas model, i.e., the enumeration of independent sets on grid graphs. We observed the influence of boundary effect and parity effect on the enumeration (or entropy), and derived upper and lower bounds for both the free energy and the first-order coefficients of boundary effects. Our computational results provided terms 0 to 3159 of the OEIS sequence A089980.

Additionally, we conducted corresponding calculations and analyses for triangular, cylindrical, and twisted cylindrical variants of grid graphs. We computed and analyzed their associated constants and compared how different adjacency and boundary conditions affect these constants. For the enumeration of independent sets on triangular grid graphs, we provided terms 0 to 40 of the OEIS sequence A027740.

## 1 Preliminary

Gaunt and Fisher [1], and Runnels and Combs [2] independently proposed the *hard-core lattice gas model* in 1965 and 1966, respectively: assume that “gas particles” are placed on the squares of an  $m \times n$  grid, and due to repulsion between particles, no two adjacent (horizontally or vertically) squares can both contain particles. Clearly, a valid configuration of  $c$  particles corresponds one-to-one with an independent (vertex) set of size  $c$  (i.e., a vertex subset with  $c$  vertices where no two vertices are adjacent) in the  $m \times n$  grid graph. The following figure is an example for an independent set with 9 vertices (the **black** vertices) of an in the  $6 \times 4$  grid graph:



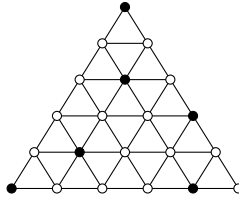
Baxter [3] analyzed this model in 1979 and proved that as the length and width  $m, n$  of the grid graph tend to infinity, the enumeration of independent sets approaches  $(e^f)^{mn}$ , where  $e^f$  is a constant called the *entropy constant* of the model, and its natural logarithm  $f$  is the *average free energy* (or *entropy per unit*) in the infinite grid graph case (the total entropy is the production of the entropy distributed by each unit). Using the transfer matrix method, Calkin and Wilf [4] calculated that:

$$1.50304808 \leq e^f \leq 1.51316067$$

Subsequent studies [5, 6] provided more precise estimates of this constant:

$$e^f = 1.5030480824753322643220663294755536893857810\ldots$$

Additionally, the lattice gas model has several simple variants. For example, replacing the  $m \times n$  grid graph with a triangular grid graph of width  $n$  (equivalent to substituting the squares of the grid with regular hexagons). The following figure is an example for an independent set with 6 vertices in the triangular grid graph with width 6:



Interestingly, the entropy constant for this variant was proven to be an algebraic number by using number theoretic methods, specifically, the unique real root of an irreducible 24th-degree polynomial [7, 8, 9]:

$$\begin{aligned} & -32751691810479015985152 + 97143135277377575190528x^4 - 73347491183630103871488x^6 \\ & - 71220809441400405884928x^8 + 107155448150443388043264x^{10} - 72405670285649161617408x^{12} \\ & + 2958015038376958230528x^{14} + 7449488310131083100160x^{16} + 797726698866658379776x^{18} \\ & + 2505062311720673792x^{20} + 2013290651222784x^{22} + 25937424601x^{24}. \end{aligned}$$

However, no similar results exist for the original grid graph.

We can also change the boundary type of the grid graph to get its variation. For example, if the horizontal *closed boundary* is changed to *periodic boundary*, that is, the vertices of the left and right sides are also connected according to the grid pattern, the *cylindrical grid graph* can be obtained.

A general method for estimating the entropy constants of such models involves expressing the independent set count as a two-dimensional tensor network contraction and computing or approximating it using the corner transfer matrix method [3, 4]. Some similar models use more complex combinatorial methods to give the upper and lower bounds in theory [10, 11]. In addition, Monte Carlo method can also be used to give approximate values [12].

In this paper, we provide exact enumerations of independent sets for small-scale grid graphs via two-dimensional tensor network contraction. In addition, we also calculate the triangular grid graphs and the variations of these graphs on the cylindrical surface.

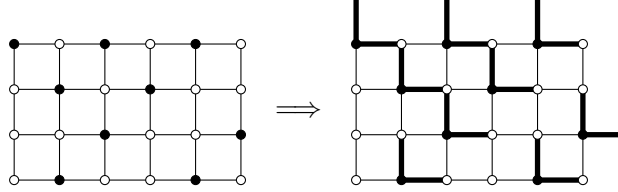
Based on these enumerations, we observe the influence of boundary effect and parity effects on the average free energy of the different models. Accordingly, we derive upper estimations for the entropy constant and the *coefficient of boundary effect* of each model.

## 2 Grid graph

We denote the number of independent sets in an  $m \times n$  grid graph as  $N(m, n)$ .

### 2.1 Algorithms

Baxter [3] provided a method to transform the enumeration of independent sets in grid graphs into a two-dimensional tensor network contraction. For convenience, we adopt an equivalent formulation here: Select (bold) the edge above and to the right of each selected point (add “half an edge” if there is no edge), then all consecutive vertices along the same diagonal will be connected, forming non-overlapping W-shaped zigzag paths. It is easy to observe that such a set of paths in an  $m \times n$  grid graph corresponds bijectively to an independent vertex set.



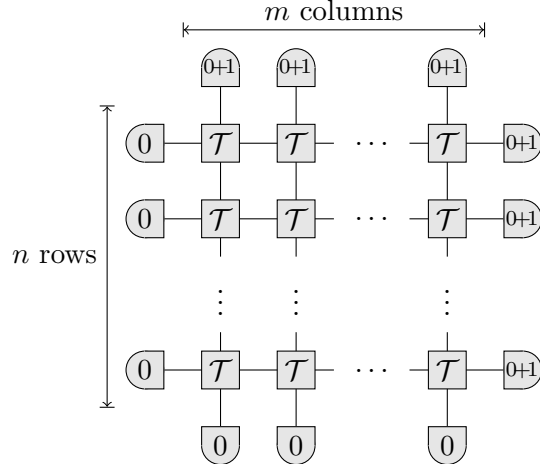
Furthermore, the edge set in the graph forms such a set of paths if and only if the connections around each vertex follow one of the following five templates (note that these templates can only assemble into W-shaped zigzag paths starting at  $\square \circ$  and ending at  $\square |$ ):

$$\square \circ, \square \circ, \square \sqcup, \square \sqcap, \square |.$$

Therefore, we define the index set  $\{0, 1\}$ , where the indices 0 and 1 represent the absence or presence of a connecting edge, respectively. The tensor  $\mathcal{T}$  of shape  $2 \times 2 \times 2 \times 2$  is constructed based on these five templates:

$$\mathcal{T} = 0 \begin{array}{c} 0 \\ \square \end{array} 0 + 1 \begin{array}{c} 0 \\ \circ \end{array} 0 + 0 \begin{array}{c} 1 \\ \sqcup \end{array} 1 + 1 \begin{array}{c} 0 \\ \circ \end{array} 0 + 0 \begin{array}{c} 0 \\ | \end{array} 0.$$

Thus,  $N(m, n)$  can be expressed as the contraction of the following two-dimensional tensor network:



Note that the tensors on the upper and right boundaries contain two indices: 0 and 1, which correspond to the two cases of no path and extended path respectively.

To reduce the memory usage, we follow the method in [13] by first contracting every four adjacent tensors, thus,

$$\begin{array}{cccccc} a_1 & a_2 & a_3 & a_4 & a_1 a_2 a_3 a_4 & a \\ \square \mathcal{T} & \square \mathcal{T} & \square \mathcal{T} & \square \mathcal{T} & \square \mathcal{T}^{(4)} & \square \mathcal{T}^{(4)} \end{array} =$$

After this contraction, the vertical indices  $a_1 a_2 a_3 a_4$  become sequences of 0s and 1s of length 4. However, only 8 (which is the size of index  $a$ ) out of the 16 possible sequences actually appear,

since no two adjacent entries in a sequence can both be 1 (otherwise, the corresponding paths would overlap). This significantly reduces the size of the state tensors that need to be stored during row-by-row contraction.

Using the congruence enumeration technique from [14], we contracted the above tensor network and computed  $N(m, n)$  for all cases where  $m + n \leq 77$ . The complete results have been archived in the corresponding OEIS sequence A089934. In addition, we also calculated all cases where  $m \leq 35, n \leq 100$ , for the next constant estimation.

## 2.2 Observation of results

We define the *average free energy* of the finite grid graph cases as:

$$f^-(m, n) := \frac{\ln N(m, n)}{(m+1)(n+1)},$$

$$f(m, n) := \frac{\ln N(m, n)}{mn}.$$

Here  $(m+1)(n+1)$  and  $mn$  are the areas under two different definitions.

Note that there are two ways to assemble  $rs$   $m \times n$  grid graphs into a larger grid graph:

(1) The graphs of  $r$  rows and  $s$  columns are directly spliced together. This can obtain all the independent sets of a  $rm \times sn$  grid graph, but the selected vertex set after splicing may not form an independent set.

(2) Add rows and columns of unselected vertices at all joints to form a  $(rm+m-1) \times (sn+n-1)$  grid graph. This can ensure that the selected vertices can form an independent set after splicing, but it can not get all the independent sets of the a  $(rm + m - 1) \times (sn + n - 1)$  grid graph.

So  $f^-(m, n)$  and  $f(m, n)$  approach to the constant  $f$  from the lower and upper sides respectively:

**Proposition 2.1.**

$$f^-(m, n) < f < f(m, n);$$

$$\lim_{m,n \rightarrow \infty} f^-(m, n) = f = \lim_{m,n \rightarrow \infty} f(m, n).$$

Which can be used to give the lower and upper bounds of  $f$ .

The charts below present the values of  $f(m, n)$  and  $f^-(m, n)$  derived from our results for some specific cases:

**Chart 2.2.1.**  $f(m, n), f^-(m, n)$  for fixed  $m$ .

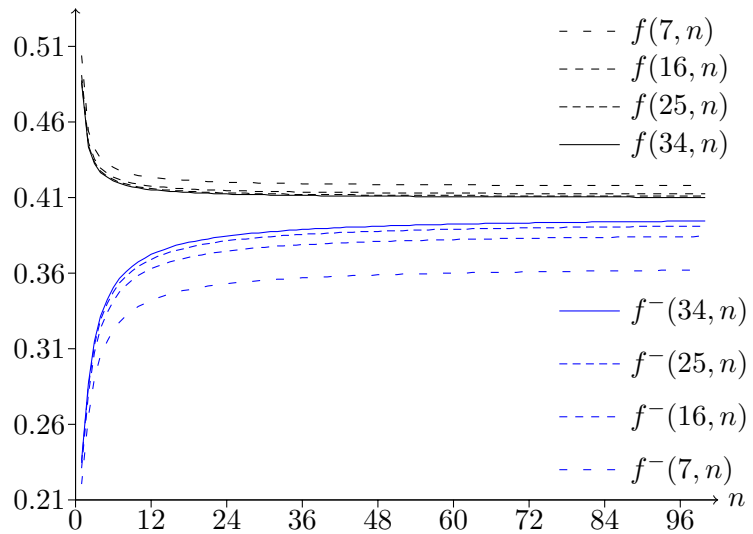


**Chart 2.2.2.**  $f(m, n), f^-(m, n)$  for fixed  $\frac{n}{m}$ .

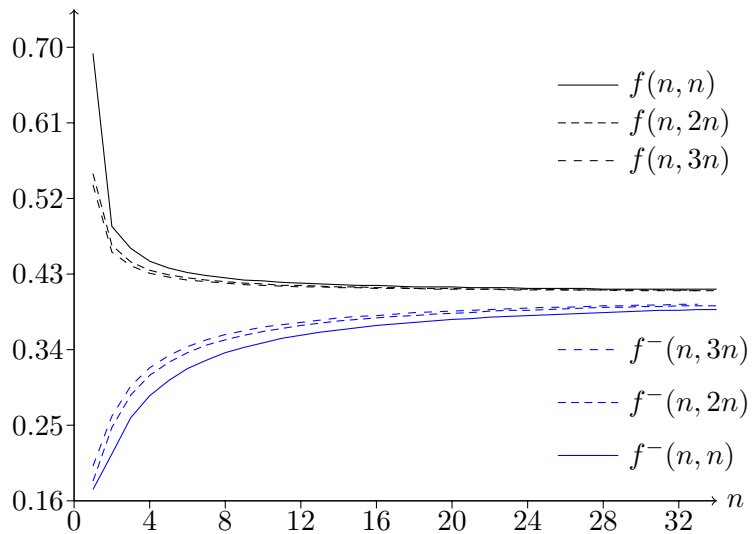
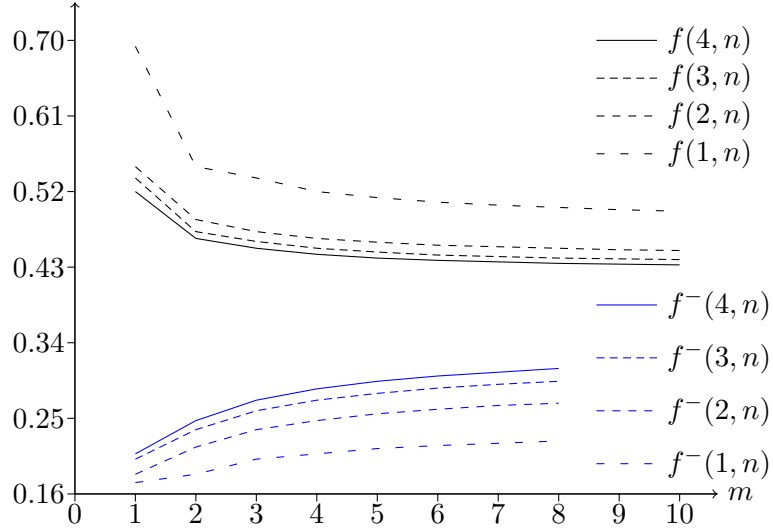


**Chart 2.2.3.**  $f(m, n), f^-(m, n)$  for smaller  $m, n$ .



It can be observed that the average free energy of the model is primarily influenced by two effects:

(1) Boundary effect: The average free energy density is larger for smaller grid sizes. This is because an  $m \times n$  grid graph can be viewed as partitioning an infinite  $\infty \times \infty$  grid graph into an  $m \times n$  region. In contrast, the infinite grid relaxes adjacency restrictions along the partition boundaries, thereby increasing the entropy contribution from vertices near the boundary. As  $m$  and  $n$  tend to infinity, this increment is approximately proportional to the “density” of boundary vertices,  $\frac{m+n}{mn}$ .

(2) Parity effect: Having an odd length or width leads to a *slightly* higher entropy compared to even dimensions, and this effect is compounded when both dimensions are odd. This occurs because, along edges of odd length, vertex selections can utilize space more “efficiently” than in even-length cases. In a sense, this effect almost only affect the area on the corner, because the existence of any a vertex on the boundary is equivalent to “reset” the parity of the boundary. Therefore, the parity effect is significant only when both the width and the height are small enough.

In summary, as  $m, n \rightarrow \infty$ , the average free energy has the asymptotic form:

$$\begin{cases} f(m, n) \sim f + k \cdot \frac{m+n}{mn} + o\left(\frac{m+n}{mn}\right), \\ f^-(m, n) \sim f + k^- \cdot \frac{m+n+2}{(m+1)(n+1)} + o\left(\frac{m+n+2}{(m+1)(n+1)}\right) \end{cases}, m, n \rightarrow \infty, \quad (1)$$

where  $k, k^-$  are the *coefficient of (first-order) boundary effect*, which can be defined as

$$k := \lim_{m, n \rightarrow \infty} \frac{f(m, n) - f}{\frac{m+n}{mn}}$$

$$k^- := \lim_{m, n \rightarrow \infty} \frac{f^-(m, n) - f}{\frac{m+n+2}{(m+1)(n+1)}}$$

### 2.3 Constant estimates

We will only give the estimation process of the constants of the version whose area is defined as  $mn$ , because the  $f$  under the two definitions is the same, and:

**Proposition 2.2.**  $k^- = f + k$ .

*Proof.* Let  $m = n$  in the definitions, thus,

$$k = \lim_{n \rightarrow \infty} \frac{n}{2}(f(n, n) - f)$$

$$k^- = \lim_{n \rightarrow \infty} \frac{n+1}{2}(f^-(n, n) - f) = \lim_{n \rightarrow \infty} \frac{n+1}{2}\left(\frac{n^2}{(n+1)^2}f(n, n) - f\right).$$

By combining the two equations, we can get

$$k^- = \lim_{n \rightarrow \infty} \frac{n+1}{2}\left(\frac{n^2}{(n+1)^2}f(n, n) - \left(f(n, n) - \frac{2}{n}k\right)\right)$$

$$= \lim_{n \rightarrow \infty} \left(\frac{2n+1}{2(n+1)}f(n, n) + \frac{n+1}{n}k\right)$$

$$= f + k$$

□

This can give another meaning of the constant: we can prove that if we define the area as  $(m+s)(n+s)$ , the corresponding boundary effect coefficient will become  $sf + k$ . So as long as

$$s = -\frac{f}{k}$$

is taken, the first-order boundary effect will become 0, which means that the boundary effect is almost negligible in the model.

To compute the two constants in this approximation, we first consider the average free energy of an  $m \times \infty$  grid graph, where  $\infty$  denotes either unidirectional or bidirectional infinite extension (the two cases are equivalent). The definition is:

$$f(m, \infty) := \lim_{n \rightarrow \infty} f(m, n) = \frac{1}{m} \lim_{n \rightarrow \infty} \frac{\ln N(m, n)}{n}.$$

And for each fixed  $m$ , we definite the boundary effect coefficient that ignoring the upper and lower boundaries:

$$k(m, \infty) := \lim_{n \rightarrow \infty} \frac{f(m, \infty) - f}{\frac{1}{n}}.$$

That is, only the left and right boundaries are considered, and the density is  $\frac{1}{n}$ .

Here we use the results of  $m \leq 35, n \leq 100$  for numerical analysis. We take data from two adjacent points and calculate the intercept and slope of their corresponding line:

$$\tilde{f}(n, \infty)(m, n) := \frac{\ln N(m, n+1)}{n+1} + k(m, \infty)(n) \cdot \frac{1}{n+1};$$

$$\tilde{k}(n, \infty)(m, n) := \frac{\frac{\ln N(m, n+1)}{(n+1)} - \frac{\ln N(m, n)}{n}}{\frac{1}{n+1} - \frac{1}{n}},$$

to approach  $f(m, \infty)$  and  $k(m, \infty)$ , respectively.

Due to the existence of parity effect, the estimation of the constants given in this way always approaches the exact value from both sides according to the parity of the selected points, so that we can give the upper and lower bounds of the constants, as shown in the **black** curves in the following figures (more precise results are provided in Appendix A):

**Chart 2.3.1.**  $f(m, \infty)$  and  $f_{\Delta}(m, \infty)$ .

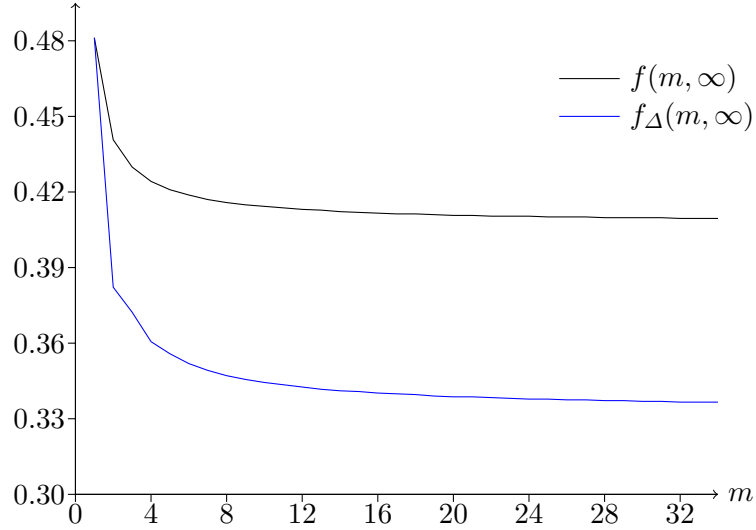
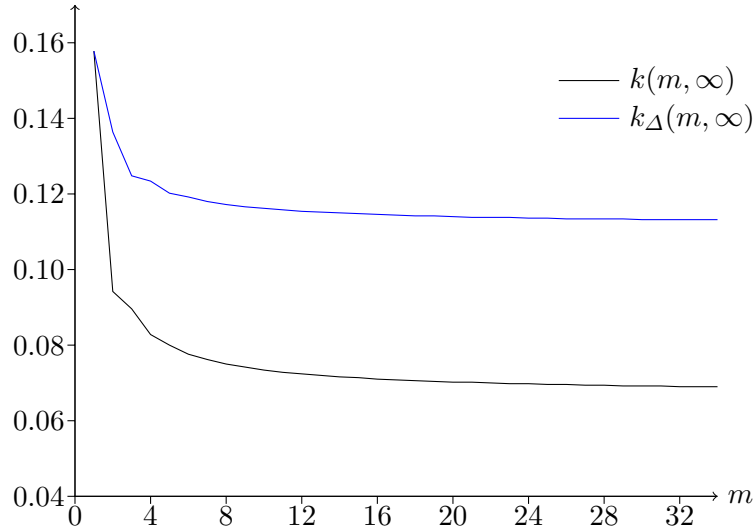


**Chart 2.3.2.**  $k(m, \infty)$  and  $k_{\Delta}(m, \infty)$ .



We can obtain the upper and lower bounds of  $f$  and  $k$  by using the same method and letting  $m \rightarrow \infty$ :

$$0.407495101260688000450146812\ 3584 < f < 0.407495101260688000450146812\ 9046;$$

$$1.5030480824753322643220663\ 2947 < e^f < 1.5030480824753322643220663\ 3030;$$

$$0.0670552316597760242912072\ 6308 < k < 0.0670552316597760242912072\ 7191.$$

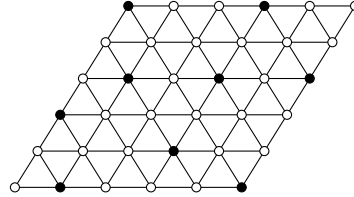
The OEIS sequence A085850 records a more accurate result of  $e^f$  (which is called the *entropy constant*), which is

$$e^f = 1.5030480824753322643220663\ 294755536893857810\dots,$$

This shows that our estimate of  $f$  is consistent with the results given by OEIS A085850 (but not so accurate). However, there is no known results of the boundary effect coefficient  $k$  has been found before us.

### 3 Triangular grid graph

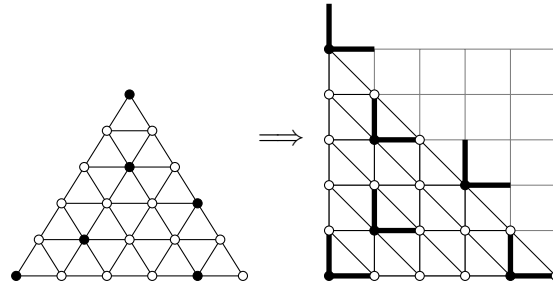
We denote the number of independent sets in a triangular grid graph of width  $n$  as  $\Delta(n)$  (similarly, the width  $n$  refers to the number of vertices along an edge). Additionally, we denote the number of independent sets in a parallelogram-shaped triangular grid graph with width  $m$  and oblique side length  $n$  (we call this a  $m \times n$  triangular grid graph) as  $\Delta(m, n)$ . An example of an independent set with 9 vertices in a  $6 \times 4$  grid graph is shown below.



The triangular grid graph of width  $n$  can be embedded into the lower-right half of an  $n \times n$  square grid graph. Thus, it is equivalent to removing the upper-left half of the vertices from the  $n \times n$  grid and adding edges connecting vertices that are adjacent along the anti-diagonal direction.

#### 3.1 Algorithms

Following the approach in the previous section, for an independent set, we still select (bold) the edges above and to the left of each chosen vertex. The selected edges form non-overlapping L-shapes, which is the shortest W-shaped path, as the diagonal edges restrict the length of the paths.

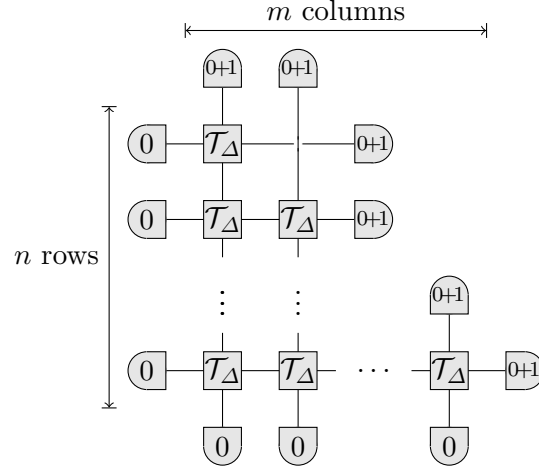


To construct such paths, we simply remove template  $0 \begin{smallmatrix} 0 \\ \square \\ 1 \end{smallmatrix} 1$  from the original set, resulting in:

$$\mathcal{T}_\Delta = 0 \begin{smallmatrix} 0 \\ \square \\ 0 \end{smallmatrix} 0 + 0 \begin{smallmatrix} 0 \\ \square \\ 0 \end{smallmatrix} 1 + 1 \begin{smallmatrix} 1 \\ \square \\ 0 \end{smallmatrix} 0 + 0 \begin{smallmatrix} 0 \\ \square \\ 1 \end{smallmatrix} 0.$$

Using this tensor, we assemble a triangular tensor network (that is, we remove the upper-right

portion of the original tensor network above the main diagonal):



and perform contractions to compute the independent set enumeration for triangular grid graphs. We have computed  $\Delta(n)$  for all  $n \leq 40$ , as shown below:

$n$	$\Delta(n)$
1	2
2	4
3	14
4	60
5	384
6	3318
7	40638
8	689636
9	16383974
10	542420394
11	25075022590
12	1617185558560
13	145563089994148
14	18283036276489970
15	3204638749437865046
16	783848125594781710150
17	267554112823378352976752
18	127443077148875066680607128
19	84712319011734340415085039268
20	78578236089316041630019193434422
21	101714646181932428248143602163208738
22	183734270908002233538130445637069602550
23	463150704646224649764463441631672026117820
24	1629220855732511492546360589163007528597792818
25	7997662422640270345091847114662902040439259297230
26	54786259684899846896275667859221962961228132566989930
27	523727899753149125104090756892359851817431315918615464448
28	6986589768922932982460178301569366275362668129029032113312408
29	130061947420267580631034025397303863700114859605321589571656334012
30	337878639320560978034291024997871301805264267270171296788786464547490
31	122488889131163566432769056089046373073543507850377415047294050165791213246
32	619666604535412306015914499142744511353655840972017434447326315502681041276430
33	437466740912168684635280144032063074869975883499801881532911772844870242164856276474
34	43098030681722787528219169313523445964284147519200826607903974311372797812802875833039502
35	592509457129279709636964362288778915586767858322153336830583272755048543979459806470418956568
36	1136733404268645896674115362009195933978738542430435519788898362676587037502096685634287527216101776
37	304331869314329106476376132792082263561735057542101942691083735979066663899507450187178239886474017129262
38	11370032865908905105623580153131121524450101592511271633433453796597634278716541353621840952593885649619259026
39	5927908367565998088617147807836324455492210314239451114540011340057177851844108442007401890743518018775086303890120
40	43128734868728759732177228362983646007805350143316692609628166393492392639713173807759187796449840239360082182539803733482

These results are also available in the corresponding OEIS sequence A027740.

### 3.2 Constant estimates

The variation trend of  $\Delta(m, n)$  is extremely close to  $N(m, n)$ , so we can use the method in the previous chapter to define and estimate the average free energy and boundary effect coefficient:

$$\begin{aligned} f_\Delta(m, n) &:= \frac{\ln \Delta(m, n)}{\frac{m+n}{mn}}; \\ f_\Delta &:= \lim_{m, n \rightarrow \infty} f_\Delta(m, n); \\ k_\Delta &:= \lim_{m, n \rightarrow \infty} \frac{f_\Delta(m, n) - f_\Delta}{\frac{m+n}{mn}}. \end{aligned}$$

and similarly perform numerical analysis using the results for all cases where  $m \leq 35, n \leq 100$  (the algorithm is similar to that of  $N(m, n)$ , just replace the tensor  $\mathcal{T}$  with  $\mathcal{T}_\Delta$ ), obtained the upper and lower bounds:

$$\begin{aligned} 0.33324272197618188785374776 \ 3953 &< f_\Delta < 0.33324272197618188785374776 \ 4006; \\ 1.395485972479302735229500663 \ 4939 &< e^{f_\Delta} < 1.395485972479302735229500663 \ 5675; \\ 0.11182308857658 \ 5958 &< k_\Delta < 0.11182308857658 \ 6865. \end{aligned}$$

and the precise value of  $e^f$  (which can be obtained by solving the polynomial) is

$$e^{f_\Delta} = 1.395485972479302735229500663 \ 566888\dots$$

which is consistent with our results.

Likewise, we can define the corresponding constants for the one-sided infinite case:

$$\begin{aligned} f_\Delta(m, \infty) &:= \lim_{n \rightarrow \infty} f_\Delta(m, n); \\ k_\Delta(n, \infty) &:= \lim_{n \rightarrow \infty} \frac{f_\Delta(m, \infty) - f_\Delta}{\frac{1}{n}}. \end{aligned}$$

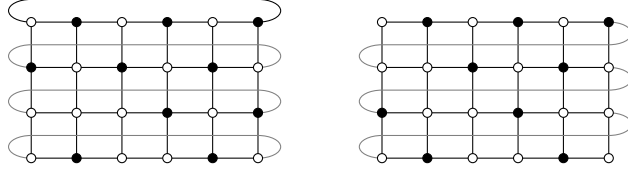
The **blue** curves in Chart 2.3.1. and Chart 2.3.2. show the values for these constants (more precise results are given in Appendix A): Through comparison, it can be clearly seen that the change trend of the corresponding constants of the two kinds of grid graphs is roughly the same, but converges to different values. Because the new edge strengthens the restriction on independent sets, the average free energy of a grid graph is always smaller than that of a triangular grid graph of the same size (when  $m, n > 1$ ), and its boundary effect coefficient is always larger.

## 4 Cylindrical grid graph

We denote the enumeration of independent sets on an  $m \times n$  cylindrical grid graph (with periodic boundary conditions in the horizontal direction) as  $C(m, n)$ .

Additionally, we consider the *twisted cylindrical grid graph*: when connecting the horizontal boundaries, we shift them by one unit. The number of independent sets on such a graph is denoted  $\Gamma(m, n)$ .

The following figures are examples of the independent sets on a cylindrical grid graph and a twisted cylindrical grid graph:



The algorithms for cylindrical and twisted cylindrical cases is given in [14], that is, splicing the tensor network in the same way, and the tensor on the remaining boundaries remains unchanged.

Following the approach in the previous chapter, we define the corresponding constants  $f_C(m, n)$  and  $f_\Gamma(m, n)$  (including the cases of  $m = \infty$  or  $n = \infty$ ). However, since the boundary conditions now differ in the two directions, the boundary effect coefficients must also be direction-dependent. Because the boundary types in the two directions are different at this time, it is also necessary to distinguish the directions of the boundary effect coefficient. Here we use the free energy of the vertically infinite case  $f_C(m, \infty)$  and  $f_\Gamma(m, \infty)$  to define the horizontal (left and right) boundary effect coefficient:

$$k_{C1}(m, n) := \frac{f_C(m, \infty) - f_C}{\frac{1}{m}};$$

$$k_{\Gamma 1}(m, n) := \frac{f_\Gamma(m, \infty) - f_\Gamma}{\frac{1}{m}}.$$

For the vertical (upper and lower) boundaries, we define them as:

$$k_{C2}(m, \infty) := \lim_{n \rightarrow \infty} \frac{f_C(m, n) - f_C(m, \infty)}{\frac{1}{n}};$$

$$k_{C2} := \lim_{m \rightarrow \infty} k_{C2}(m, \infty);$$

$$k_{\Gamma 2}(m, \infty) := \lim_{n \rightarrow \infty} \frac{f_\Gamma(m, n) - f_\Gamma(m, \infty)}{\frac{1}{n}};$$

$$k_{\Gamma 2} := \lim_{m \rightarrow \infty} k_{\Gamma 2}(m, \infty).$$

Under these definitions, we have:

$$\begin{aligned} f_C(m, n) &= f_C(m, \infty) + k_{C2}(m, \infty) \cdot \frac{1}{n} + o(\frac{1}{n}) \\ &= f_C + k_{C1} \cdot \frac{1}{m} + k_{C2} \cdot \frac{1}{n} + o(\frac{1}{\min\{m, n\}}) \\ &= f_C + k_{C1} \cdot \frac{1}{m} + k_{C2} \cdot \frac{1}{n} + o(\frac{1}{\min\{m, n\}}); \\ f_\Gamma(m, n) &= f_\Gamma(m, \infty) + k_{\Gamma 2}(m, \infty) \cdot \frac{1}{n} + o(\frac{1}{n}) \\ &= f_\Gamma + k_{\Gamma 1} \cdot \frac{1}{m} + k_{\Gamma 2} \cdot \frac{1}{n} + o(\frac{1}{\min\{m, n\}}) \\ &= f_\Gamma + k_{\Gamma 1} \cdot \frac{1}{m} + k_{\Gamma 2} \cdot \frac{1}{n} + o(\frac{1}{\min\{m, n\}}); \end{aligned}$$

Note that the (twisted) cylindrical grid graph of size  $m \times n$  can also be assembled by splicing an  $m \times n$  grid graph, so, similar to Proposition 2.1., we can define:

$$f_C^-(m, n) := \frac{\ln C(m, n)}{(m+1)n};$$

$$f_\Gamma^-(m, n) := \frac{\ln \Gamma(m, n)}{(m+1)n},$$

Note that the area definition of the “-” version here is  $(m+1)n$  rather than  $(m+1)(n+1)$ , because there is no splicing in the vertical direction. And we have:

**Proposition 4.1.**

$$f_C(m, n) < f_C < f_C^-(m, n);$$

$$\lim_{m,n \rightarrow \infty} f_C(m, n) = f_C := \lim_{m,n \rightarrow \infty} f_C^-(m, n).$$

$$f_\Gamma(m, n) < f_\Gamma < f_\Gamma^-(m, n);$$

$$\lim_{m,n \rightarrow \infty} f_\Gamma(m, n) = f_\Gamma = \lim_{m,n \rightarrow \infty} f_\Gamma^-(m, n).$$

Substituted these into the inequalities in Proposition 2.1., we get:

$$f^-(m, n) < f_C(m+1, n) < f(m+2, n);$$

$$f^-(m, n) < f_\Gamma(m+1, n) < f(m+2, n),$$

and,

**Corollary 4.1.**

$$f(\infty, n) = f_C(\infty, n) = f_\Gamma(\infty, n).$$

This can also be considered that when the width is infinite, the grid graphs on the three faces are equivalent.

These easily lead to:

**Corollary 4.2.**

$$f = f_C = f_\Gamma.$$

Following the previous process, we calculate all cases with  $m \leq 31, n \leq 91$  and perform numerical analysis. Some results of the cylindrical case are saved in the corresponding OEIS sequence A286513. The following charts show the case of  $n = \infty$ :

**Chart 4.1.** Comparison of  $f(m, \infty)$ ,  $f_C(m, \infty)$  and  $f_\Gamma(m, \infty)$ .

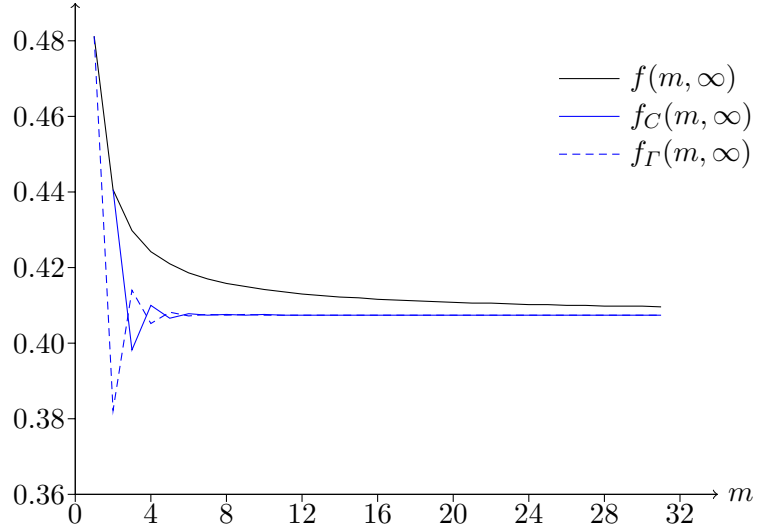
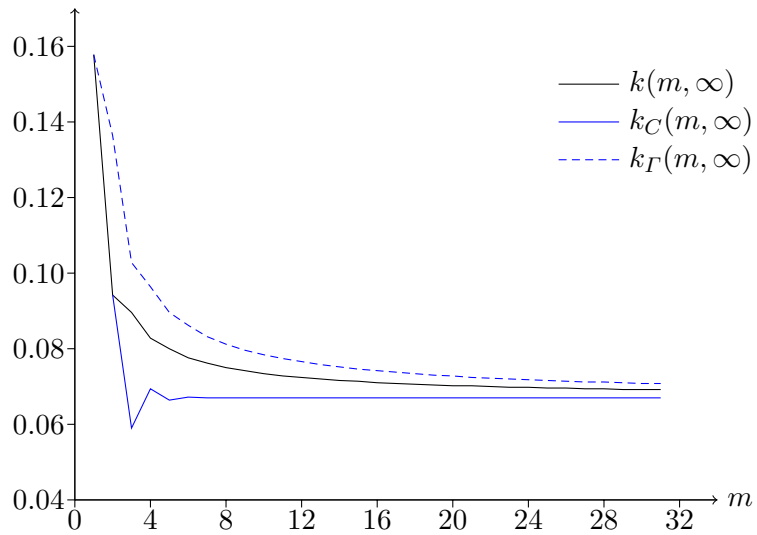


**Chart 4.2.** Comparison of  $k(m, \infty)$ ,  $k_{C2}(m, \infty)$  and  $k_{\Gamma 2}(m, \infty)$ .

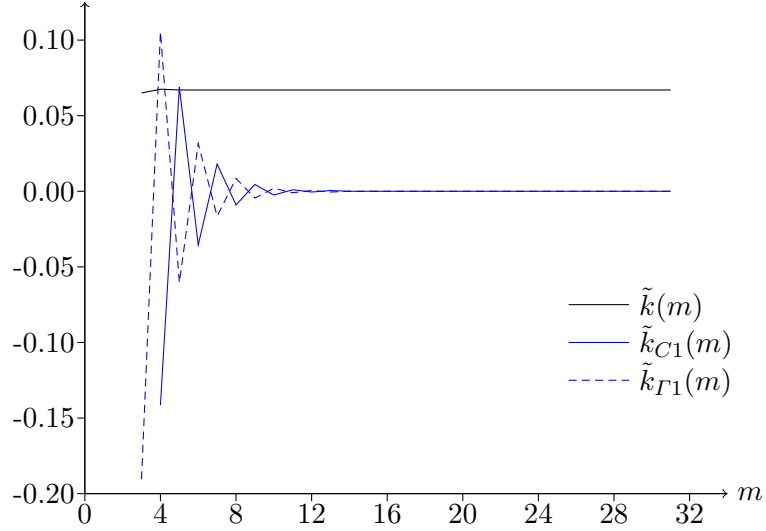


And here we use

$$\begin{aligned}\tilde{k}_{C1}(m) &:= \frac{f(m, \infty) - f(m-1, \infty)}{\frac{1}{m} - \frac{1}{m-1}}; \\ \tilde{k}_{\Gamma 1}(m) &:= \frac{f(m, \infty) - f(m-1, \infty)}{\frac{1}{m} - \frac{1}{m-1}},\end{aligned}$$

to approach  $k_{C1}, k_{\Gamma 1}$ .

**Chart 4.3.** Comparison of  $\tilde{k}(m)$  (define in a similar way),  $\tilde{k}_{C1}(m)$  and  $\tilde{k}_{\Gamma 1}(m)$ .



Based on these results, we can observe that:

- (1) The horizontal boundary effect coefficients in cylindrical and twisted cylindrical cases are most likely all zero, meaning there is no first-order boundary effect.
- (2) Such periodic boundary conditions can only reduce first-order boundary effect but cannot diminish higher-order boundary effect (i.e., the remainder term  $o(\frac{m+n}{mn})$ ).
- (3) There are still parity effects on the cylinder and twisted cylinder, but the intensity and phase will change.

The following are the upper and lower bounds of the constants given by the results:

$$0.407495101260\ 6521 < f_C < 0.407495101260\ 7636;$$

$$1.503048082475\ 2784 < e^{f_C} < 1.503048082475\ 4459;$$

$$-0.000000000000\ 1581 < k_{C1} < 0.000000000000\ 3415;$$

$$0.0670552316597\ 6690 < k_{C2} < 0.0670552316597\ 7922;$$

$$0.4074951012606\ 1207 < f_\Gamma < 0.4074951012606\ 8296;$$

$$1.503048082475\ 2181 < e^{f_\Gamma} < 1.503048082475\ 3858;$$

$$-0.000000000000\ 3500 < k_{\Gamma 1} < 0.000000000000\ 1625.$$

$$0.068\ 1077 < k_{\Gamma 2} < 0.068\ 6918.$$

The results of free energy here are all in accordance with Corollary 4.2..

In addition, it can be seen that the horizontal (periodic) boundary effect coefficients of cylindrical and twisted cylindrical cases are close to (probably equal to) 0, but the vertical boundary effect coefficients defined in our way have obvious differences: the vertical boundary effect coefficients of cylindrical cases are close to (probably equal to) the original plane cases, but those of twisted cylindrical cases are slightly larger.

In fact, the convergence speed of the relevant data of  $k_{\Gamma 2}$  is significantly slower, which makes the distance between the upper and lower bounds larger. But after more careful calculation,  $k_{\Gamma 2}$  is indeed greater than  $k_{C2}$  or  $k$ . This shows that the upper and lower boundaries of the spiral cylinder are not equivalent to those of the cylinder (from the first-order boundary effect), although there is

little difference between them (only the upper left corner and the lower right corner each have an additional horizontal boundary of unit length).

This phenomenon may explain that the combinatorial properties of the hard-core lattice gas model lead to some *instability*: small changes in boundary conditions will still have a significant impact on large-scale.

## References

- [1] David S. Gaunt and Michael E. Fisher. Hard-sphere lattice gases. i. plane-square lattice. *Journal of Chemical Physics*, 43(8):2840–2863, 1965.
- [2] Runnels and K. L. Exact finite method of lattice statistics. i. square and triangular lattice gases of hard molecules. *Journal of Chemical Physics*, 45(7):2482–2492, 1966.
- [3] R. J. Baxter, I. G. Enting, and S. K. Tsang. Hard-square lattice gas. *Journal of Statistical Physics*, 22(4):465–489, 1980.
- [4] Neil J. Calkin and Herbert S. Wilf. The number of independent sets in a grid graph. *Siam Journal on Discrete Mathematics*, 11(1):54–60, 1998.
- [5] R. J. Baxter. Planar lattice gases with nearest-neighbor exclusion. *Annals of Combinatorics*, 1999.
- [6] Steven R. Finch. Several constants arising in statistical mechanics. *Annals of Combinatorics*, 3(2):323–335, 1999.
- [7] G., S., and Joyce. On the hard-hexagon model and the theory of modular functions. *Philosophical Transactions of the Royal Society A Mathematical Physical & Engineering Sciences*, 1988.
- [8] Moore and M A. Exactly solved models in statistical mechanics. *Physics Bulletin*, 34(4):167, 1983.
- [9] George E. Andrews. *The reasonable and unreasonable effectiveness of number theory in statistical mechanics*. The reasonable and unreasonable effectiveness of number theory in statistical mechanics, 1992.
- [10] S. Forchhammer and J. Justesen. Entropy bounds for constrained two-dimensional fields. *IEEE Transactions on Information Theory*, 45(1):118–127, 1999.
- [11] Shmuel Friedland and Uri N. Peled. Theory of computation of multidimensional entropy with an application to the monomer-dimer problem. *Advances in Applied Mathematics*, 2005.
- [12] Isabel Beichl and Francis Sullivan. Approximating the permanent via importance sampling with application to the dimer covering problem. *Journal of Computational Physics*, 149(1):128–147, 1999.
- [13] Kai Liang. Independent set enumeration in king graphs by tensor network contractions, 2025.
- [14] Kai Liang. Solving tiling enumeration problems by tensor network contractions, 2025.

## A Constants for $m \times \infty$ cases

The “error” in the following chart refers to the distance between the value shown and the upper and lower bounds.

Grid graph:

$m$	$f(m, \infty)$	error
1	0.481211825059603447497758913424368423135184334385_-	1.747e-82
2	0.44068679350977151261630466248986154514080164130_-	1.254e-148
3	0.429871029469374617950502914215407621751493746077_-	1.357e-73
4	0.424257111068728554960881148611310343385770258391_-	3.886e-85
5	0.4209063075918052590652822971338741852067557428_-	3.992e-62
6	0.418670960739873749692906536419297297610417504662_-	1.446e-70
7	0.417074421385321816780333443033043436788244381734_-	8.010e-52
8	0.415877005130446830774849291812225853508277913251_-	8.448e-59
9	0.414945682569572652037471297844666328527191144 2_-	5.682e-47
10	0.414200624426308363715217595712867744428405846193_-	2.674e-53
11	0.4135910314117670017779892681925885053004945 0484_-	3.020e-44
12	0.413083037232346002699682398392625715616382528413_-	3.174e-49
13	0.41265319600375189977128148105026539246011 4976_-	1.440e-42
14	0.412284760664958275459409226752805875605855128 52_-	1.451e-46
15	0.41196545003806530869127760198135177550 7070_-	1.775e-41
16	0.41168605323942402459214147892923319517674846 246_-	9.756e-45
17	0.4114395266524395359156223124434991281951 2778_-	9.592e-41
18	0.411220391908453336021773745187698496657393 1669_-	1.952e-43
19	0.411024323979623580854538130414925550812 5065_-	3.044e-40
20	0.4108478628367680170021684745069597390548 8288_-	1.740e-42
21	0.410688207530201144471188690913678349738 1433_-	6.731e-40
22	0.41054306633613236519210888233021034550034 8147_-	8.851e-42
23	0.41041054611546087107180008510273441637 9154_-	1.154e-39
24	0.4102890692465120014623411967975378700895 1127_-	3.013e-41
25	0.41017731052707904142180761867366231500 1098_-	1.639e-39
26	0.410074148632217847538272582175709542277 9113_-	7.633e-41
27	0.4099786283591982235720439158977028677 1656_-	2.021e-39
28	0.409889930962822858460547184220356642248 3511_-	1.549e-40
29	0.40980735062826648404639536242542927385 1737_-	2.236e-39
30	0.409730275649347201259853726325633945829 8986_-	2.651e-40
31	0.40965817324971303349179866085301097279 0761_-	2.277e-39
32	0.409590577250056001209247039801263134634 3196_-	3.972e-40
33	0.4095270797765091027715309334898084721 6025_-	2.181e-39
34	0.409467313956563765870476437990537859488 9704_-	5.363e-40
$m$	$k(m, \infty)$	error
1	0.157704693902156707695138160235643026507568 1627_-	1.713e-43
2	0.094113203229798857907688601760807807476330096950_-	1.567e-75
3	0.089590595253620610958483031556189783985 0744_-	9.287e-40
4	0.082706110770076437664639784430276786124850714074_-	3.307e-50
5	0.0799636657371019442359679068953730957 7545_-	3.502e-38
6	0.07768286319536690360481487669446424868260 3315_-	1.220e-44
7	0.076210158016163396359992393664850599 9250_-	1.350e-37
8	0.07504915109469166499659477811134949817217 7525_-	1.282e-42
9	0.074167201449674311189331903680694397 1554_-	2.395e-37
10	0.0734535917564779054479654972801765690803 7262_-	3.897e-41
11	0.072872869750062939058794970820749162 0830_-	2.990e-37
12	0.072387688911533138399641388409320558971 3772_-	6.629e-40
13	0.071977652512398651078419678585251967 2498_-	3.119e-37
14	0.07162598863572782535655686417696289485 7281_-	3.317e-39
15	0.071321297261801034384744194035040107 1100_-	2.948e-37
16	0.07105465743353447688935973036592269292 8693_-	9.278e-39
17	0.070819401596965957635253329296005247 0737_-	3.729e-37
18	0.070610279141644379239757778616521266 2653_-	1.840e-38
19	0.0704231721888167902821970140296235 3504_-	2.987e-37
20	0.0702547748162389155593212775996855676 7132_-	2.924e-38
21	0.070102415767128742205132772972078911 7743_-	2.127e-37
22	0.0699639073434227980050260540626556 2622_-	3.988e-38
23	0.06983744320453931831080970574661624 5808_-	1.232e-37
24	0.0697215177093714253647846816922009571 5198_-	7.604e-38
25	0.069614866272691741257826344293937 2269_-	3.659e-35
26	0.0695164187852539187271538693626759707 6526_-	8.090e-38
27	0.0694252637075554206289884555248855134 2813_-	3.224e-38
28	0.0693406197053978042029012221213195930 5661_-	7.901e-38
29	0.0692618132212655882751137793392571195 3206_-	7.420e-38
30	0.0691882605024607765257384775377960059 2528_-	7.091e-38
31	0.0691194531204780203570578461962257885 6314_-	9.503e-38
32	0.0690549461998313561746290663562608670 7103_-	5.823e-38
33	0.0689943487895172154034152171991675924 6264_-	9.867e-38
34	0.0689373159327566231401134135441448806 1161_-	4.318e-38

## Triangular grid graph:

$m$	$f_{\Delta}(m, \infty)$	error
1	0.481211825059603447497758913424368423135184334385..	1.747e-82
2	0.38224508584003564132935849918485739375941641 915..	3.349e-45
3	0.372185143199076763266438568096490403101529933154..	2.819e-49
4	0.3607372594505253932356497619912931246474689208 0..	2.230e-47
5	0.35574260139400142667383872264604317138623503951 ..	6.381e-48
6	0.351838510551468457327336830230539179770776192 18..	1.091e-46
7	0.3492304710973854521753183718551848532972884234 0..	8.923e-47
8	0.347216425333764595019305431779792865100194 23..	2.694e-46
9	0.345668874361900112165909451684223000385211678 27..	9.082e-46
10	0.344424579960030349578661266569394297742112559 87..	4.340e-46
11	0.34340860776006355731375982848042383722602510 15..	8.011e-46
12	0.34256126206381766309302250075389279069756298 73..	8.093e-46
13	0.3418445151749295896587401049344373088696597 4372..	1.001e-44
14	0.34123007959877623106055112000280299170447600 018..	1.569e-45
15	0.34069759655121014213426871695280823289617100 637..	7.458e-45
16	0.34023166432283304403008842353019848544135116 989..	6.473e-45
17	0.3398205509541514536439138349684883168071509 4929..	1.284e-44
18	0.3394551157034229582635409277398703885069682 4781..	3.265e-44
19	0.3391281477194529652638295786705659963786269 8875..	3.405e-44
20	0.33883387639498084558089899709528124848592 1676..	4.486e-43
21	0.338567630959519888013826215503303318356141 1154..	2.462e-43
22	0.338325589637527454336559674309339012930534 2153..	6.331e-43
23	0.338104595392985880697595795767070906878520 3133..	2.382e-43
24	0.337902017333388166149907579935765553552723 4030..	7.134e-43
25	0.337715645519298739666219293958362935060086 3543..	7.564e-43
26	0.33754360999833945353622915781621265905764 5568..	1.430e-42
27	0.33738431784939546073229378761077942603728 5567..	2.436e-42
28	0.337236403711105762413099245829477556477482 3970..	3.248e-42
29	0.33709869054778915895037690262621621525631 5198..	7.484e-42
30	0.33697015826206781234582488981430152444752 1126..	7.663e-42
31	0.336849918381878336075080903206734706364 7320..	2.019e-41
32	0.336737193494200182578633629884835534715 8657..	1.781e-41
33	0.336631300417896475414730549578153917682 9039..	4.406e-41
34	0.3365316363460814898609100974438130774421 4908..	3.951e-41
$m$	$k_{\Delta}(m, \infty)$	error
1	0.157704693902156707695138160235643026507568 1627..	1.713e-43
2	0.136318375996289851824900656377108616529558 6145..	2.942e-43
3	0.124779734547815277575328401242676768879648440946..	1.657e-49
4	0.12340128633760295349358663830804577211694463 471..	1.964e-45
5	0.120269670957925531231970554977389421840926019 90..	5.806e-46
6	0.11919010179930900780970428779547415049113528 862..	9.437e-45
7	0.11801051816905876235207899422347042425553638 001..	7.825e-45
8	0.1172855408621138041544067145812395978210482 2096..	2.109e-44
9	0.1166602842871648936642580154725193435103388 2812..	8.216e-44
10	0.1161834562799485167860292613123980064093115 9213..	3.813e-44
11	0.1157844771411471693625783131620706642506280 4907..	7.089e-44
12	0.1154553251984579630498524072687294586420934 7530..	7.098e-44
13	0.115175563804177121239701172335088404939898 0421..	9.557e-43
14	0.114936234376557618379573906366753118180169 5803..	1.379e-43
15	0.114728642090003165045569858243177810498211 4506..	6.466e-43
16	0.114547063171153367928106540098894313891609 7504..	5.706e-43
17	0.11438682262232187740068207289391332953340 4823..	1.124e-42
18	0.1142443954468862641734634141735610648952 4933..	2.899e-42
19	0.11411695732242368356953819768221990334652 7526..	3.003e-42
20	0.1140022642248757471196083330967720102360 6188..	4.195e-41
21	0.1138984938306209342425785042848056594528 5284..	2.437e-41
22	0.113804157274347022038082376328123361201 2767..	5.128e-41
23	0.1137180238356884460676627683959065914150 5011..	2.094e-41
24	0.1136390682061608161437306020812945788215 8048..	6.209e-41
25	0.1135664290186695165669693571728736934614 6456..	6.673e-41
26	0.113499377464054630448090685602368756819 8238..	1.251e-40
27	0.113437292690131898901798507927305962124 4462..	2.156e-40
28	0.113379642543343679915539864493437664232 3510..	2.850e-40
29	0.113325968268576876549615889259872726360 5232..	6.645e-40
30	0.113275872278859448989700868142222172987 4146..	6.741e-40
31	0.1132290082884578206898143924993444526 8575..	1.797e-39
32	0.11318507329746395365313807764011883336 1099..	1.569e-39
33	0.11314380103319416877820268162892073932 2538..	3.921e-39
34	0.11310495654917658496510327263170924234 5723..	3.471e-39

## Cylindrical grid graph:

$m$	$f_C(m, \infty)$	error
1	0 (the only independent set is $\emptyset$ )	0
2	0.440686793509771512616304662489896154514080164130-	1.251e-129
3	0.398254405762369768037310276173030174512054025051-	1.741e-174
4	0.410056037580579286727537638792521264389586605666-	2.139e-100
5	0.406614574980743081640389836200888915263352129819-	2.033e-147
6	0.407805573398536382991903920818913345252317984757-	1.342e-85
7	0.407377738577143243451221510847062650686604173598-	8.335e-98
8	0.407540536130730140731839318252510680906485802109-	5.210e-85
9	0.407476963681491300463330442585951099346721397808-	1.295e-86
10	0.407502471475487026435527618723306480058269230819-	8.362e-88
11	0.4074920542551040916475126610265319801278556-	1.230e-85
12	0.407496377100376185384519327125170551732763696616-	7.995e-88
13	0.407494560965162970545768569350680042886730654216-	2.953e-88
14	0.40749533219553774090668410468130049793076448197-	9.131e-82
15	0.407495001749216172449207026695309846175670097667-	4.803e-88
16	0.407495144440752752741969695175287476323400224471-	1.609e-77
17	0.407495082408498643751305339031118807868850953304-	4.176e-85
18	0.407495109536104074790465042795975811149297052744-	1.283e-74
19	0.407495097610523111547294519582805426452560404542-	5.537e-81
20	0.407495102877685270603811366618664293414579011448-	1.450e-72
21	0.407495100541578208244421788140535724922803069607-	6.013e-78
22	0.407495101581617887126121171542424854050914030074-	4.497e-71
23	0.407495101117001368589640269493627537165536599329-	1.174e-75
24	0.407495101325207882306455345585423473932062789344-	5.734e-70
25	0.407495101231638639587932465274376676688491194070-	6.773e-74
26	0.407495101273799510554827159084124619267373898347-	3.898e-69
27	0.407495101254756563506359230289825949211319186169-	1.609e-72
28	0.407495101263376965740585753999796650834757405018-	1.678e-68
29	0.407495101259466585205452618291974879303603309567-	1.972e-71
30	0.407495101261243822574379032361490716480249123388-	5.152e-68
31	0.40749510126043633484484050423978390730211167124-	1.463e-70
$m$	$k_C(m, \infty)$	error
1	-	-
2	0.094113203229798857907688601760807870476330096950-	1.353e-68
3	0.058928544290683157847990049517066671735428179528-	1.187e-91
4	0.06938413541442289573672196551543584972360350817-	1.050e-87
5	0.066349971797211572898678998542916885396729949589-	1.119e-86
6	0.06727128336683671933109952381397714627897082687-	1.566e-75
7	0.066990956574619982750578768491331448486517499317-	5.186e-87
8	0.067073487883750124065906408790421520135592315860-	4.958e-69
9	0.06705080753962847417655663879607747603984151538-	1.366e-83
10	0.06705875265203839591691111087583241250917952574-	2.574e-66
11	0.067055449697414623250926893674904138368831987764-	2.645e-76
12	0.067054939670252881058575824970385362679783027662-	5.759e-65
13	0.067055439843000970264267785735087829089945918016-	3.688e-72
14	0.067055107004958819081878953863174320845937647593-	3.152e-64
15	0.067055300559273677912863560564681415520385524124-	1.353e-69
16	0.067055195268804030622893454747952449219041017221-	8.415e-64
17	0.067055250342055383438047886787789777632224661100-	6.534e-68
18	0.06705522251013947991134430036066893905291095666-	1.509e-63
19	0.067055236334463331290766044870984517693129973-	9.321e-67
20	0.067055229360003603776196466269453314968536147662-	2.135e-63
21	0.067055237287700178096060954299026089317479646-	6.122e-66
22	0.06705523114536093633528215212248391815161374633-	2.609e-63
23	0.067055231923324108412205910254879476862377664872-	2.403e-65
24	0.06705523153283687141123141319643440912450410544-	2.898e-63
25	0.067055231720744515806079458731005688214044471962-	6.613e-65
26	0.067055231630560092651377513594770571366742143632-	3.009e-63
27	0.067055231673750133496731804564530192471753485104-	1.417e-64
28	0.067055231653102360943547136134394664015312947581-	8.365e-65
29	0.067055231662959172577426601984300852713008382333-	2.528e-64
30	0.067055231658259336594700238327482607097573034216-	7.931e-65
31	0.06705523166049806068591304747903978998646042007-	3.935e-64

## Twisted cylindrical grid graph:

$m$	$f_\Gamma(m, \infty)$	error
1	0.481211825059603447497758913424368423135184334385_-	1.405e-72
2	0.382245085840035641329358499184857393759 9528_-	5.604e-40
3	0.414012737393791820480636815310017557854610176308_-	1.500e-58
4	0.405232530750285635920785757404854484 2433_-	6.908e-37
5	0.408262736040184546339178363369158329655654535391_-	7.088e-55
6	0.4072089041212947542796448691827240907 4923_-	4.511e-38
7	0.40760365191996157595052614862499321445378952 710_-	1.465e-45
8	0.40745230426117547228714011564303725 7489_-	2.817e-36
9	0.4075122784136574422746986216416979839852 2082_-	2.940e-41
10	0.40748806545781566840651037600958582 7281_-	4.209e-36
11	0.4074980228174302011291109972989459438 7985_-	3.767e-39
12	0.40749387251157802338470925220543239 2773_-	9.634e-36
13	0.407495623290421691691825048139826966 6609_-	1.459e-37
14	0.4074948774836853669704182351097 1814_-	1.113e-34
15	0.407495197916042828879887388842156205 5684_-	5.478e-37
16	0.4074950592325462032251082556333721 1745_-	2.053e-35
17	0.40749511642721045506031199830406827038 3071_-	1.540e-40
18	0.4074950931789316017287723036442312 4241_-	1.030e-35
19	0.40749510483037793950781920406055174 0841_-	2.098e-36
20	0.40749509967738423226957820070549119 1107_-	6.190e-36
21	0.40749510196559278378638787842427569 5780_-	5.625e-36
22	0.40749510094578393311477133823361481 8958_-	5.328e-36
23	0.40749510140180398191472021063304281 7259_-	9.032e-36
24	0.40749510119727040826175954171464828 4602_-	3.419e-36
25	0.4074951012892624732647558002423677 5919_-	1.126e-35
26	0.40749510124778196643608751950843079 4434_-	1.984e-36
27	0.4074951012665301765391613403951012 9041_-	1.203e-35
28	0.407495101258037954011910461509730 3125_-	9.804e-34
29	0.40749510126118923885098172621609952 3968_-	1.165e-35
30	0.407495101260139651511182830118599665 6187_-	6.058e-37
31	0.4074951012609380777207571160790426 5801_-	1.059e-35
$m$	$k_\Gamma(m, \infty)$	error
1	0.15770469390215670769513816023564302650 6455_-	1.115e-39
2	0.1363183759962898518249006563771086164 8877_-	4.273e-38
3	0.1028839094970235649388951420136 4985_-	2.434e-32
4	0.0963321941406637583409596322217173 8855_-	5.470e-35
5	0.0895037738579192436201670970140 7304_-	4.831e-32
6	0.08613280214930877189772928060128008 7592_-	4.624e-36
7	0.0832393794842196232484907743150 8427_-	2.507e-32
8	0.081292607133394605050859350090584 6305_-	2.659e-34
9	0.0796746833693701006564375117036 9931_-	1.305e-32
10	0.078429729752766003836701729121272 3180_-	4.828e-34
11	0.07738760588704182332852943875801 4238_-	7.745e-33
12	0.07653041129038867063504518408986 7596_-	1.195e-33
13	0.07579972866455769075168507084123 5474_-	5.119e-33
14	0.0751759865484192639602342694855 5154_-	1.007e-32
15	0.07463419288035277780688542518522 5090_-	3.672e-33
16	0.07416070199674430628571883048783 1323_-	2.077e-33
17	0.073742641248427884963411101101896 0927_-	3.734e-33
18	0.07337116195888578690249822523960 0690_-	1.338e-33
19	0.07303872402948985530039850387460 3937_-	2.720e-33
20	0.07273955911801600596667522391781 0327_-	1.124e-33
21	0.07246887227338439145329223494973 1612_-	1.837e-33
22	0.07222279986488635598716249250623 4946_-	1.033e-33
23	0.0719981219643762907318864215370 9460_-	1.126e-33
24	0.071792168684124835999300774090616 6339_-	9.708e-34
25	0.071602690975435200770622940464770 9202_-	6.319e-34
26	0.07142778880154401904731237615774 9053_-	1.263e-33
27	0.071265842190007563383607180292365 4795_-	2.828e-34
28	0.0711154632664453495151334446257 9546_-	1.141e-33
29	0.070975455268704619873307686350058 5193_-	1.649e-34
30	0.07084478115374289177499034851027 2773_-	1.008e-33
31	0.070722537619160271456433407511615 1337_-	1.310e-34